

# Bridging the Sim2Real Gap: Vision Encoder Pre-Training for Visuomotor Policy Transfer

Samuel Biruduganti<sup>\*†</sup> Yash Yardi<sup>\*†</sup> Lars Ankile<sup>‡</sup>

<sup>†</sup>Illinois Mathematics and Science Academy <sup>‡</sup>Massachusetts Institute of Technology  
{sbiruduganti, yyardi}@imsa.edu ankile@mit.edu

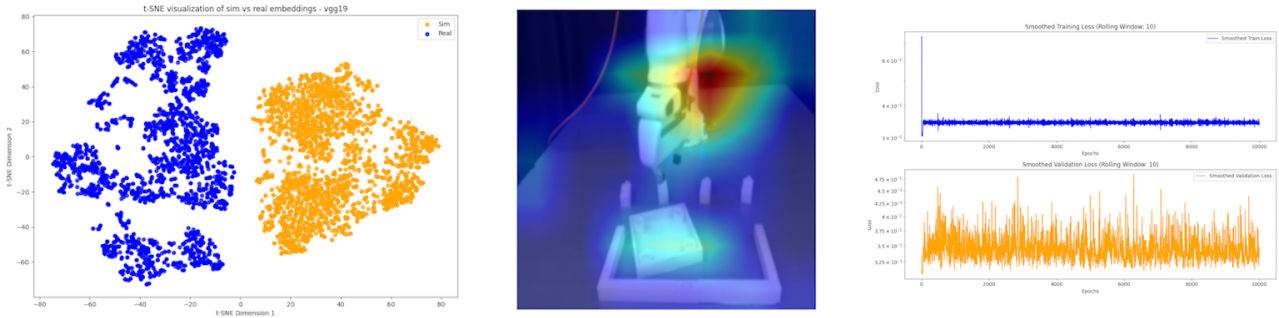


Fig. 1. An Overview of the Qualitative and Quantitative Measures Used

**Abstract**—Simulation offers a scalable and efficient alternative to real-world data collection for learning visuomotor robotic policies. However, the simulation-to-reality, or “Sim2Real” distribution shift—introduced by employing simulation-trained policies in real-world environments—frequently prevents successful policy transfer. This study explores the potential of using large-scale pre-training of vision encoders to address the Sim2Real gap. We examine a diverse collection of encoders, evaluating their ability to (1) extract features necessary for robot control while (2) remaining invariant to task-irrelevant environmental variations. We quantitatively measure the encoder’s feature extraction capabilities through linear probing and its domain invariance by computing distances between simulation and real-world embedding centroids. Additional qualitative insights are provided through t-SNE plots and GradCAM saliency maps. Findings suggest that encoders pre-trained on manipulation-specific datasets generally outperform those trained on generic datasets in bridging the Sim2Real gap. <https://github.com/yyardi/Bridging-the-Sim2Real-Gap>

## I. INTRODUCTION

Robots that can reliably function in unstructured environments, like a home or construction site, operating from vision alone, have the potential to transform daily life and industry [1]. Visuomotor robotic policies—algorithms that enable robots to perform tasks solely using image observations are necessary to accomplish this. Recent advancements have been made using Neural Networks (NNs) and machine learning to learn these policies from data [2]–[4]. However, gathering the vast data necessary for robots to learn robust policies on physical robots is often impractical and can pose safety risks.

Simulation is a scalable alternative that has allowed researchers to replicate years of robot training in a fraction of

the time [5]. Despite the incredible benefits, the simulation will inevitably differ from the real environment. This difference introduces a distribution shift known as the Sim2Real gap, which, if not adequately addressed, results in poorly performing simulation-trained policies when deployed in real settings.

A promising way to improve the Sim2Real gap is to pre-train visual representations [6]. These neural networks, trained on enormous datasets, convert raw images into compact, information-rich representation vectors that improve transferability by preferably extracting task-relevant information. This study assesses various encoders’ potential for transfer learning of visuomotor policies. We hypothesize that effective vision encoders capable of bridging the Sim2Real gap should (1) pick out relevant features from an image to infer actions (e.g., the objects and their position) and (2) ignore task-irrelevant parts of the image that change between simulated and real environments (e.g., the table color and clutter objects).

To comprehensively understand the potential for the vision encoders to (1) predict the correct actions based on the image and (2) to neglect domain-specific features that vary between simulated and real environments, we employ various quantitative and qualitative metrics described in detail in Section 3.

We find that the type of pre-training data used, either manipulation-specific data or general image data, tends to be the most important factor in determining an encoder’s overall performance. We also found that CNN-based encoders generally outperformed ViT-based encoders in domain invariance. We present our findings as a 2-dimensional plot according to our two criteria.

\*Equal Contribution

## II. RELATED WORKS

Given the significant potential of AI-enabled robots capable of real-world unsupervised operation, many researchers have explored the nature of and potential solutions to the Sim2Real gap. Training machine learning models to help robots learn visuomotor policies traditionally requires enormous datasets that are costly and time-consuming to produce. Thus, it is crucial to solve the problem of increasing the viability of robots with diversely applicable visuomotor policies in the future.

### A. Pre-Trained Visual Representations

The robotics research community has investigated pre-trained visual representations (PVRs) for training downstream policies in real-world tasks, comparing their performance across simulated and real environments. PVRs produce embeddings (output features of 1-dimensional vectors) extracted from visual data using pre-trained vision encoders designed for visuomotor tasks. Silwal et al. conducted a comprehensive investigation into using PVRs for training policies, evaluating their effectiveness in simulated and real environments [7]. The study demonstrated that PVRs significantly improved Sim2Real transfer in the ImageNav task compared to previous methods.

Burns et al. further studied the success of PVRs in robotic manipulation tasks, focusing on the attributes of pre-trained vision models robust to distribution shifts, including subtle lighting and texture changes [8]. The study evaluates fifteen models to identify which features made them more reliable under these conditions. The authors found that models pre-trained on manipulation-relevant data could consistently generalize better than models trained on standard pre-training datasets like ImageNet [9]. Notably, they found that a model’s strong emergent segmentation ability—the capacity to separate essential parts of an image from irrelevant details naturally—showcased its consistent success in generalization despite distribution shifts. Given the significant relevance of these distribution shifts to the Sim2Real gap, this finding applies directly to this inquiry’s application of the PVRs in examining whether the nature of the model’s pre-training indicates its performance.

### B. Custom Frameworks for Learning to Generalize

To combat the distribution shift, a study introduced Maniwhere, a framework to improve generalization across diverse visual disturbances [10]. Maniwhere leverages multi-view representation learning with a Spatial Transformer Network to extract meaningful information from varying viewpoints. By combining a fixed image with a randomly perturbed one, the model learns correspondences that enhance its ability to generalize semantic features. Then, reinforcement learning is employed to train the robot through environmental interaction, optimizing its decision-making process. Evaluated on eight manipulation tasks, the unique framework demonstrated superior visual generalization and Sim2Real transfer compared to other designs. This study’s multi-view

approach highlights a promising avenue for addressing the Sim2Real gap in future research.

### C. Probing to Evaluate Quality of Learning

The robotics community continues to explore cost-efficient methods for evaluating learned representations in training visuomotor policies. Linear probing is an affordable alternative to experimental assessments with reinforcement learning (RL) algorithms introduced in [11]. Researchers applied this approach in the Arcade Learning Environment, testing nine Atari games by comparing actions predicted by the probes to those taken by RL algorithms. The probes estimated task-specific rewards and identified optimal actions, with results showing a strong correlation between probe predictions and RL performance. This method proved to be up to 600 times more computationally efficient than RL-based evaluations. These findings validate this research’s novel probing to predict the action-inference performance of surveyed models without requiring direct experimentation on robots.

## III. METHODS

We evaluate several pre-trained vision encoders’ ability to learn effective visuomotor policies transferable to real-world applications. We posit that to tackle the Sim2Real gap, effective encoders should exhibit high action-inference accuracy—indicating relevant feature extraction ability—and low source determination ability, or high domain invariance, thus minimizing the Sim2Real gap. Encoder attributes are assessed by generating embeddings, using linear probes and distance metrics for quantitative comparison, and performing qualitative analyses with t-SNE plots and Grad-CAM saliency maps on image samples [12,13]. With matching action and domain labels, the image dataset includes more than 50,000 frames of a robot arm trying to construct a small table—a challenging task—from simulated and real—world settings [14,15]. This large collection offers a solid basis for assessing encoder generalization across domains because it contains a variety of situations, such as different illumination and object layouts.

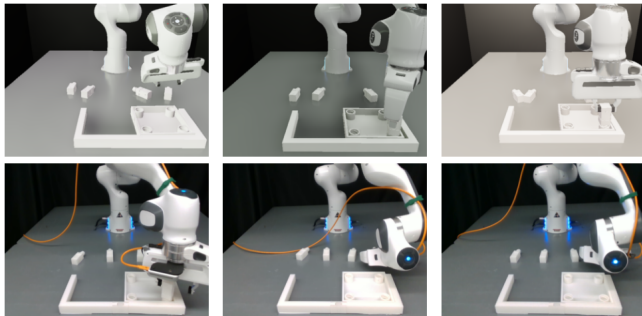


**Fig. 2.** Three Random Frames from the Dataset used. Top Row is Simulation Images; Bottom Row is Real Images. To the human eye, the simulated and real scenes are visually highly similar. Still, machine learning systems struggle.

TABLE I. Overview of Pre-trained Vision Encoders included in the study

No.	Model Name	Architecture	Embedding Dim	Parameters (M)	Training Type	Pre-Training Data
1	CLIP-Base-16	Transformer	512	51	Self-supervised	General
2	CLIP-Base-32	Transformer	512	151	Self-supervised	General
3	CLIP-Large-14	Transformer	768	432	Self-supervised	General
4	DinoV2-B	Transformer	768	86	Self-supervised	General
5	EfficientNet B0	CNN	1280	5.3	Supervised	General
6	HRP-ResNet18	CNN	512	11.7	Supervised	Manipulation
7	HRP-ViT	Transformer	768	24	Supervised	Manipulation
8	MCR	CNN	2048	5.9	Self-supervised	Robot Manipulation
9	MobileNetV3	CNN	1280	5.4	Supervised	General
10	MVP	Transformer	768	43	Self-supervised	Manipulation
11	R3M ResNet18	CNN	512	11.7	Self-supervised	Manipulation
12	R3M ResNet34	CNN	512	21.3	Self-supervised	Manipulation
13	R3M ResNet50	CNN	2048	25.6	Self-supervised	Manipulation
14	ResNet18	CNN	512	11.7	Supervised	General (ImageNet)
15	ResNet34	CNN	512	21.3	Supervised	General (ImageNet)
16	ResNet50	CNN	2048	25.6	Supervised	General (ImageNet)
17	ResNet101	CNN	2048	44.6	Supervised	General (ImageNet)
18	Swin Transformer	Transformer	1024	87	Self-supervised	General
19	VC1-B	CNN	768	22.6	Self-supervised	General
20	VGG16	CNN	4096	138	Supervised	General
21	VGG19	CNN	4096	143	Supervised	General
22	VIP	CNN	1024	22.6	Self-supervised	Manipulation
23	Vision Transformer (ViT)	Transformer	768	86	Supervised	General (ImageNet)

A. The Encoders

A vision encoder is a function  $f_\theta : R^{H \times W \times C} \rightarrow d_z$  that maps an image  $x_i \in R^{H \times W \times C}$  with height and width being 240 by 320 in our case, and the standard three channels for RGB. The output  $f_\theta(x_i)$  is a 1-dimensional vector  $z_i \in R^{d_x}$  which is supposed to be a low-dimensional, information-dense representation of the contents of the image.

Twenty-three encoders are analyzed across all procedures to evaluate the performance of various model architectures in the Sim2Real gap, making this study contain, to our knowledge, the largest number of models examined in any study within this field [16]–[29]. Using action probing (Sec. 3.D), centroid distance (Sec. 3.C), t-SNE [12] (Sec. 3.E), and GradCAM [13] (Sec. 3.F), we explore how well models can discover relevant features for predicting visuomotor policies and how well models generalize their learning. Our encoder selection provides a broad and representative sampling of contemporary visual representation learning approaches, spanning multiple neural network structures, training methodologies, and datasets useful for training more robust models. Each encoder is categorized into Convolutional Neural Networks (CNNs) [30] and Vision Transformers (ViTs) [31]. CNNs are traditional approaches to image analysis designed to learn and extract features from images hierarchically. Alternatively, ViTs treat inputs like puzzles, relating pieces to create a holistic view of the image. We also compare models pre-trained on different data sets, some using manipulation datasets like Ego4D [32], and others using general data sets like ImageNet [9], to see if this pre-training data impacts Sim2Real performance. A complete list of the encoders is provided in Table 1, including architectural type, training approach, and size.

B. Generating Embeddings (Passing Images with Neural Networks)

We use each encoder to generate and store embeddings for all sim and real-world images. Embeddings are vector representations of the observed images the encoders generate, abstractly demonstrating learned representations and extracted features from the image. When fed an image, the neural networks convert the data into abstract vectors representing the image. These numbers are then passed through the layers of the neural networks that compress the data into smaller dimensions and perform calculations on it. The embeddings can be passed through an action prediction model to predict actions and learn visuomotor policies. Each pre-trained vision encoder will process images differently due to fundamental differences in the neural network designs, processing methods, and learned weights, demonstrating varying performance in our thorough qualitative and quantitative procedures. All model embeddings are normalized to ensure analyses are on the same scale across all benchmarks [33].

C. Quantitatively Evaluating Domain Invariance With Centroid Distance Metric

We quantify each encoder’s domain invariance using a centroid distance metric, which measures the average difference between encoder-learned representations of pictures from simulated and actual environments to compare the extent of the Sim2Real gap. This approach (1) uses Principal Component Analysis (PCA) [34] to project all encoders into the same embedding space despite the encoders having different-size embeddings out of the box. Then, (2) min-max normalization is used to scale embeddings between 0 and 1, ensuring that scale differences are accounted for. Min-max normalization subtracts each feature’s minimal value and

divides it by its range. (3) The embeddings are then divided into sim and real subsets, and the centroids are computed by finding the mean value for each embedding dimension for each subset. The final step (4) is the Euclidean distance calculation between sim and real centroids, measuring how closely the embeddings align. The outputted number subtracted from 1 is the “domain invariance score,” (DIS) calculated in equation (1)

$$DIS = 1 - \left\| \frac{1}{n_r} \sum_{i=1}^{n_r} z_i - \frac{1}{n_s} \sum_{i=1}^{n_s} z_j \right\|_2^2 \quad (1)$$

Here,  $\frac{1}{n_r} \sum_{i=1}^{n_r} z_i \in R^{d_x}$  is a vector of the same size as the embeddings produced by the encoder that represents the centroid of the embeddings produced from the images from the real domain, and similarly for the images from the simulated domain for the second term in the norm.

#### D. Quantitatively Evaluating Task-Relevant Information With “Action Probing”

We quantitatively analyze each encoder’s ability to infer actions with a technique we call “action probing,” based on the interpretation technique of linear probing [11]. For any given encoder to succeed in a visuomotor policy learning application, it must create embeddings with features relevant to determine what motor commands the robot should follow. The probe is a simple single-layer neural network that maps the embeddings to a prediction of the motor commands the robot should take to complete a task. The process consists of two parts: (1) training, in which we measure loss from the probe against labeled data and adjust weights accordingly for the next epoch, and (2) validation, in which the model predicts an action from held-out images to ensure the model is not purely memorizing the image features when adjusting weights.

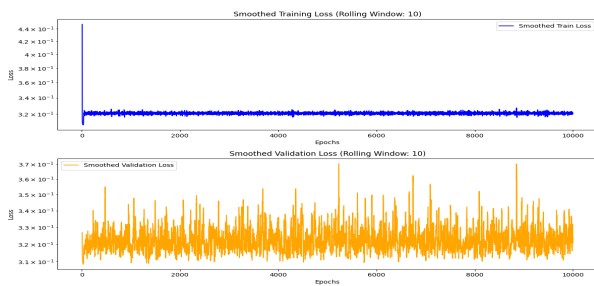


**Fig. 3.** An Example Action Probe Training Process (ResNet34).

The linear probes were run on the embeddings of each encoder over 10,000 epochs, measuring both training and validation loss, and an average of the training loss over the last 100 epochs was taken. This average loss is subtracted from one to give the “action score,” which returns a comparative, quantitative metric of the accuracy of potential motor commands from the embeddings. The action score (AS) is calculated in equation (2).

$$AS = 1 - \frac{1}{n} \frac{1}{d} \sum_{i=1}^n \sum_{j=1}^d |a_{ij} - g_\phi(z_i)_j|^2 \quad (2)$$

In (2),  $n$  is the number of data points across sim and real,  $d$  is the dimensionality of each robot action,  $a \in R^{n \times d}$  is the dataset of all the ground truth actions,  $g_{phi} : R^{d_x} \rightarrow R^d$  is the action probe function that maps the embedding vector  $z_i$  of dimension  $d_z$  for each image into a prediction of the corresponding action with parameters  $\phi$  learned using gradient ascent on the above score function.

#### E. Qualitatively Analyzing Domain Invariance with t-SNE Plotting

We use t-distributed Stochastic Neighbor Embedding (t-SNE) [12] plots to qualitatively analyze the differences between simulation-generated embeddings and real-world embeddings for each encoder based on the overlap of the plotted clusters. t-SNE is an unsupervised non-linear dimensionality reduction technique for data exploration and visualizing high-dimensional data. t-SNE-reduced clusters of the sim and real embeddings are plotted in 2-dimensions, with the presumption that less overlap between the clusters indicates encoders picking up on more spurious differences between the images. Increased distance would lead to different embeddings and, potentially, a more significant Sim2Real gap.

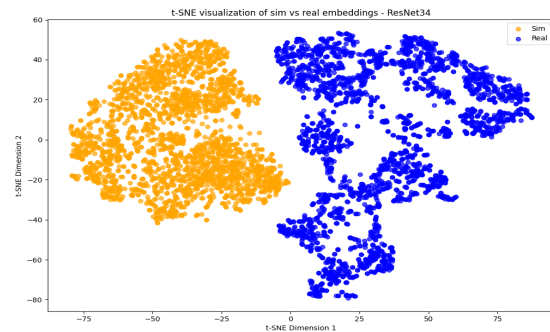


**Fig. 4.** An Example t-SNE Plot (ResNet34)

#### F. Qualitatively Understanding Encoders with GradCAM Saliency Maps

To comprehensively understand each model’s performance regarding the Sim2Real gap and their applicability in visuomotor policies, we qualitatively analyze what each model is “looking for” when given an image. As the images are converted into pixel values and passed through the model layers, the pre-trained weights will adjust them according to the target for which they have been trained (in this case, visuomotor control). GradCAM (Gradient-weighted Class Activation Mapping) is suitable for identifying the most critical regions of each input image for the learned representations [13]. These visual explanations are later compared

with quantitative metrics to analyze each encoder’s action inference and domain invariance capabilities. GradCAM works by calculating a gradient of the activations in the final layer of a neural network and then overlaying this gradient onto the input image, representing the sensitivity of different regions to altered activations in the final layer as colors. The heat map indicates which parts of the image have the most significant impact on the generated embedding, thus demonstrating what the model is paying attention to. Some characteristics we can observe are whether the model focuses on the robot or the surrounding environment (which could impact domain-invariance) and how narrow the focus of the robot is on the robot’s end-effector and the objects on the table it interacts with (impacting action-inference).

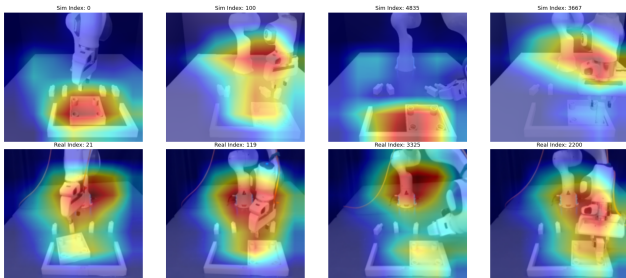


**Fig. 5.** An Example GradCAM Plot for the ResNet34 encoder, comparing visually similar images for sim (top row) and real (bottom row).

## IV. EXPERIMENTAL RESULTS

### A. Analyzing Domain Invariance - Action Inference Plot

This section outlines the results of evaluating the 23 surveyed encoders using our proposed quantitative metrics. In Figure 6, we plot the results of the centroid distance metric against the linear probing metric for each encoder to visualize their relative performance in domain invariance and action inference. CNN-based encoders are plotted in blue, while transformer-based encoders are in orange. The shape of each point indicates its form of pre-training: a circle for encoders trained on manipulation data and a square for encoders trained on general visual data. The relative size of each point represents the number of parameters in the corresponding encoder. The y-axis represents the action score, while the x-axis represents the domain invariance score, meaning being closer to 1 on both axes indicates higher performance in each metric, or that being further up and right on the plot is ideal for any given encoder.

Figure 6 demonstrates general trends regarding a given encoder’s characteristics and performance across the two metrics. A significant pattern was the relationship between pre-training data and action-inference performance. All encoders trained on manipulation data performed highly in action inference, while encoders trained on general data had mixed results. This pattern is exhibited when comparing the ResNet models (pre-trained only on ImageNet [35]) to their R3M counterparts, where R3M encoders are

ResNet-based but trained with self-supervised learning on vast amounts of publicly available manipulation data. Each R3M encoder outperformed its ResNet counterpart in both metrics. Another intriguing pattern was that, despite the general understanding that more model parameters produce more accurate results, the number of parameters didn’t seem to impact either performance metric, indicating that it doesn’t affect Sim2Real performance. As for encoder type, ViT-based encoders generally performed worse in the centroid distance metric than CNN-based encoders. According to the plot, the overall highest-performing encoder was MCR (numbered 8 on the plot) [22], a CNN-based encoder trained on manipulation data, abiding by the observed patterns. MCR is especially unique compared to other encoders because it is specifically pre-trained on robotic manipulation data, rather than human manipulation data.

### B. Comparing Quantitative Results To Qualitative Observations

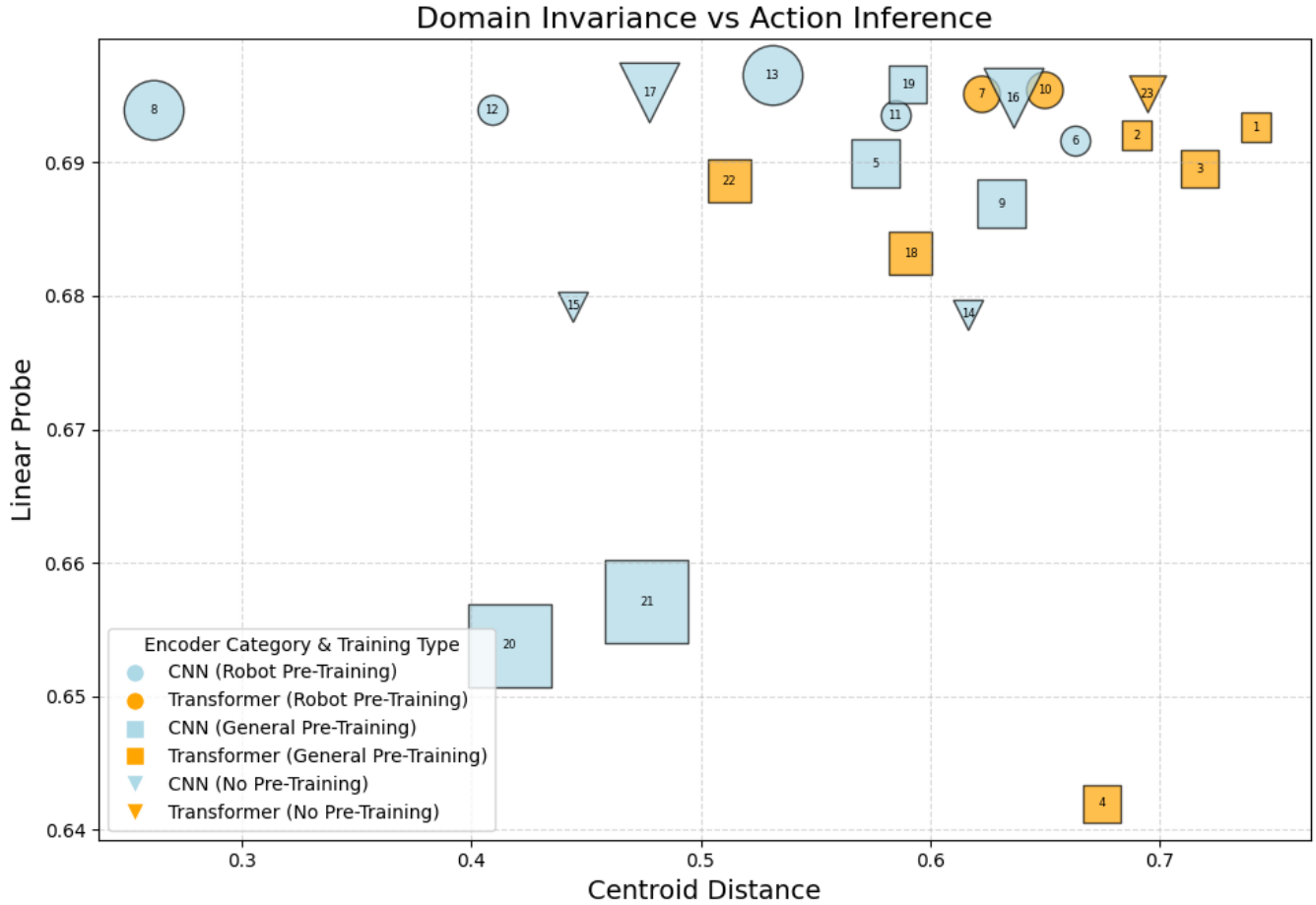
We analyze the results of our qualitative experimentation using Grad-CAM saliency maps and t-SNE plots to contextualize the performance of various encoders on the plot. For each encoder, we generated a grid of saliency maps and a t-SNE plot to observe how they relate to the encoder’s quantitative domain invariance and action inference performance. Figures 7 through 10 show the Grad-CAM maps and t-SNE plots generated from four selected models, including the overall worst-performing model (DinoV2-B), the overall best-performing model (MCR), a model with high domain invariance but low action inference ability (VGG-16), and a model with high action inference ability but low domain invariance (CLIP-Base-32).

Figure 7 shows that DinoV2-B does not have a clear focus across any of the maps, indicating low action inference performance, which corresponds with its action probe metric. Furthermore, the t-SNE plot for DinoV2-B shows a wide gap between the sim and real clusters, indicating low domain invariance, which its domain invariance score confirms.

Figure 8 shows that MCR not only has a sharp focus on the robot end-effectors and the objects in the Grad-CAM maps for both simulated and real images but also exhibits some cluster overlap in the t-SNE plot, being one of the only models to do so. This finding aligns well with its high performance in both quantitative metrics.

In Figure 9, VGG-16 demonstrates a lack of focus on any particular part of the images in the Grad-CAM maps but has a relatively small gap between sim and real clusters in the t-SNE plot, explaining how it performed relatively well in the centroid distance metric but poorly in the action probe metric.

In Figure 10, the Grad-CAM maps demonstrate that CLIP-Base-32 visualized the simulated and real images completely differently, explaining how it performed poorly in the centroid distance metric despite its low action probe loss. This is a case where the t-SNE plot does not illustrate new information as well about the model’s performance.



**Fig. 6.** Plot Of Each Encoder’s Performance In Domain Invariance and Action Inference, where point size represents the number of parameters, point color represents CNN/ViT-based, and point shape represents manipulation/general pre-training. See Table I for corresponding encoder numbers.

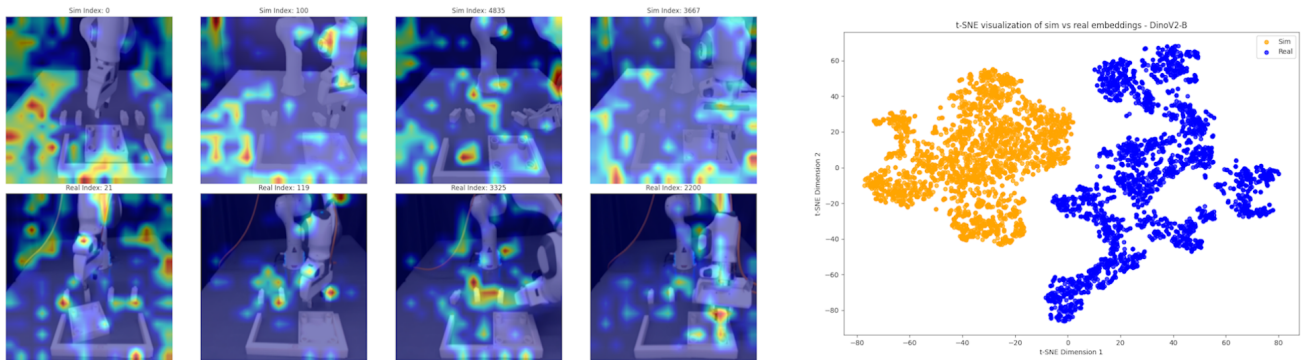


**Fig. 7.** Grad-CAM and t-SNE Plot Generated With DinoV2-B

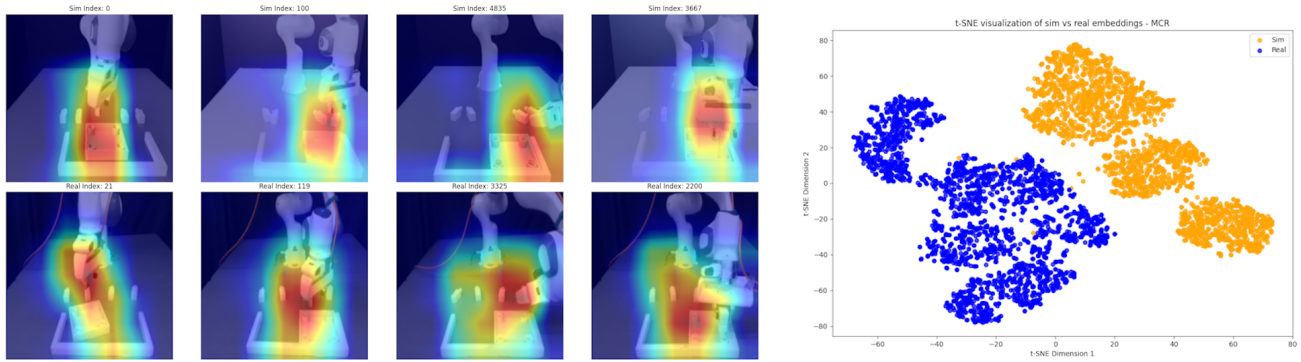


**Fig. 8.** Grad-CAM and t-SNE Plot Generated With MCR

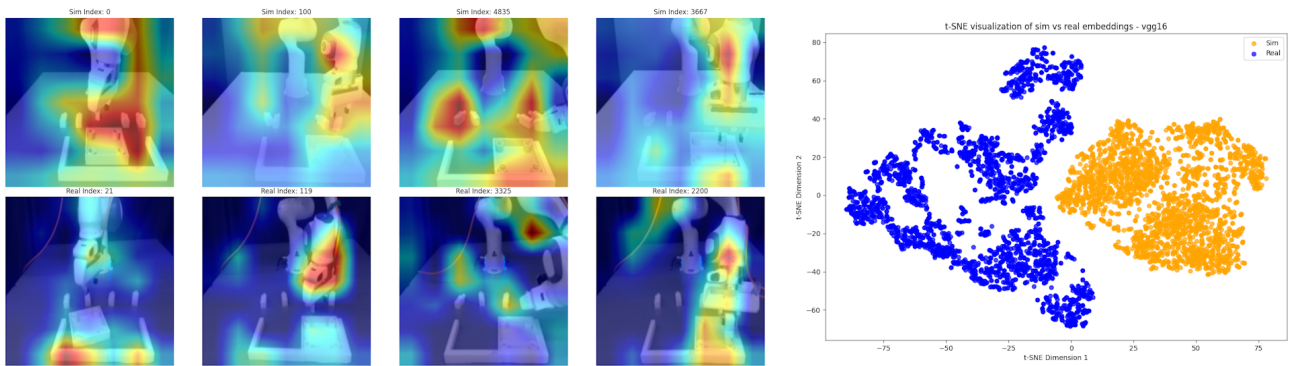


**Fig. 9.** Grad-CAM and t-SNE Plot Generated With VGG-16

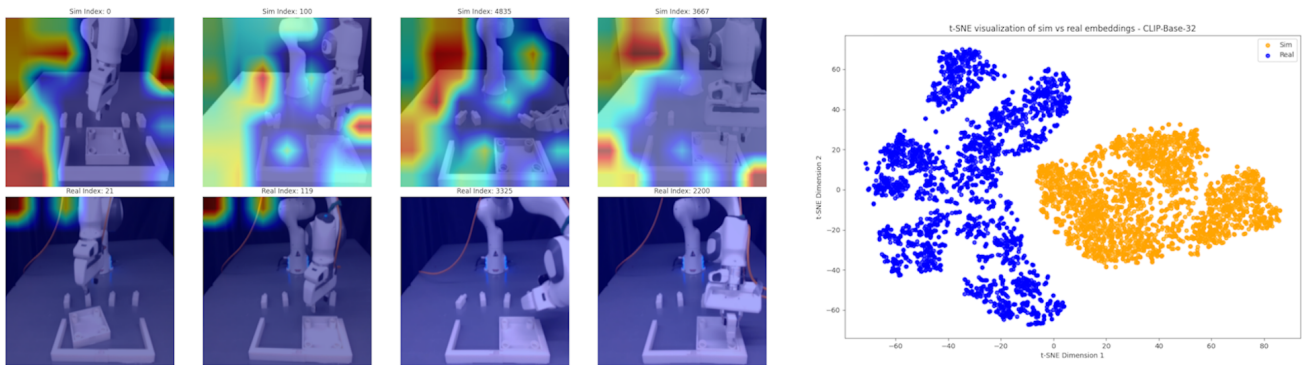


**Fig. 10.** Grad-CAM and t-SNE Plot Generated With CLIP-Base-32

## V. DISCUSSION

### A. Limitations

The relationships between quantitative results and qualitative analysis of the Grad-CAM maps and t-SNE plots were not constant across all observed encoders. The Grad-CAM maps experienced a large amount of variation, even among encoders that performed similarly in both quantitative metrics. Furthermore, several Grad-CAM maps seemed to contradict the encoder’s action probe performance, displaying a significant degree of randomness in the focus of the maps despite performing well in the action probe metric.

Additionally, the t-SNE plots rarely exhibited any overlap, even among models that performed well in the centroid distance metric. As such, both qualitative metrics should be further investigated to examine their effectiveness in determining Sim2Real performance.

### B. Future Directions

We propose that the quantitative element of the survey, using centroid distance and linear probing to observe the encoders’ abilities in domain invariance and action inference, could be turned into a database of different encoders and their corresponding performance metrics. Furthermore, this

strategy for evaluating encoders could be turned into a score method, accepting different models as inputs and outputting a Sim2Real score calculated through a cost function factoring in centroid distance and action probe performance. We also propose that future research should confirm the findings of this study through real-world experimentation, using encoders to learn transferable visuomotor policies for task completion and testing them in simulated and real environments, comparing performance to confirm their ability to bridge the Sim2Real gap.

#### ACKNOWLEDGMENTS

We sincerely thank the Massachusetts Institute of Technology Improbable AI Lab for assisting with this extensive study of pre-trained encoders. Their computational resources and sizable datasets made this possible. We also acknowledge Mr. Lars Ankile for his dedicated mentoring during this investigation. His knowledge and support were crucial in determining the course and methodology of our study. Our effort would not have been possible without their persistent support and generous contributions.

#### REFERENCES

- [1] G. A. Bekey, "On autonomous robots," p. 143–146, 1998. [Online]. Available: <https://doi.org/10.1017/S0269888998002033>
- [2] C. Chi, Z. Xu, S. Feng, E. Cousineau, Y. Du, B. Burchfiel, R. Tedrake, and S. Song, "Diffusion policy: Visuomotor policy learning via action diffusion," 2024. [Online]. Available: <https://arxiv.org/abs/2303.04137>
- [3] P. Florence, L. Manuelli, and R. Tedrake, "Self-supervised correspondence in visuomotor policy learning," pp. 492–499, 2020. [Online]. Available: <https://doi.org/10.1109/LRA.2019.2956365>
- [4] I. Radosavovic, T. Xiao, S. James, P. Abbeel, J. Malik, and T. Darrell, "Real-world robot learning with masked visual pre-training," 2022. [Online]. Available: <https://arxiv.org/abs/2210.03109>
- [5] H. Ju, R. Juan, R. Gomez, K. Nakamura, and G. Li, "Transferring policy of deep reinforcement learning from simulation to reality for robotics," pp. 1077–1087, 2022. [Online]. Available: <https://doi.org/10.1038/s42256-022-00573-6>
- [6] C. K. Clayton Fields, "Renaissance: Investigating the pretraining of vision-language encoders," 2024. [Online]. Available: <https://arxiv.org/abs/2411.06657>
- [7] S. Silwal, K. Yadav, T. Wu, J. Vakil, A. Majumdar, S. Arnaud, C. Chen, V.-P. Berges, D. Batra, A. Rajeswaran, M. Kalakrishnan, F. Meier, and O. Maksymets, "What do we learn from a large-scale study of pre-trained visual representations in sim and real environments?" pp. 17515–17521, 2024. [Online]. Available: <https://doi.org/10.1109/ICRA57147.2024.10610218>
- [8] K. Burns, Z. Witzel, J. I. Hamid, T. Yu, C. Finn, and K. Hausman, "What makes pre-trained visual representations successful for robust manipulation?" 2024. [Online]. Available: <https://openreview.net/forum?id=A1hpY5RNiH>
- [9] J. Deng, W. Dong, R. Socher, L.-J. Li, K. Li, and L. Fei-Fei, "Imagenet: A large-scale hierarchical image database," in *2009 IEEE Conference on Computer Vision and Pattern Recognition*, 2009, pp. 248–255.
- [10] Z. Yuan, T. Wei, S. Cheng, G. Zhang, Y. Chen, and H. Xu, "Learning to manipulate anywhere: A visual generalizable framework for reinforcement learning," 2024. [Online]. Available: <https://openreview.net/forum?id=jart4nhCQr>
- [11] W. Zhang, A. GX-Chen, V. Sobal, Y. LeCun, and N. Carion, "Light-weight probing of unsupervised representations for reinforcement learning," 2024. [Online]. Available: <https://arxiv.org/abs/2208.12345>
- [12] M. Balamurali, *t-Distributed Stochastic Neighbor Embedding*. Cham: Springer International Publishing, 2023, pp. 1527–1535. [Online]. Available: [https://doi.org/10.1007/978-3-030-85040-1\\_446](https://doi.org/10.1007/978-3-030-85040-1_446)
- [13] R. R. Selvaraju, M. Cogswell, A. Das, R. Vedantam, D. Parikh, and D. Batra, "Grad-cam: Visual explanations from deep networks via gradient-based localization," *International Journal of Computer Vision*, vol. 128, no. 2, p. 336–359, Oct. 2019. [Online]. Available: <http://dx.doi.org/10.1007/s11263-019-01228-7>
- [14] M. Heo, Y. Lee, D. Lee, and J. J. Lim, "Furniturebench: Reproducible real-world benchmark for long-horizon complex manipulation," 2023. [Online]. Available: <https://arxiv.org/abs/2305.12821>
- [15] L. Ankile, A. Simeonov, I. Shenfeld, M. Torne, and P. Agrawal, "From imitation to refinement – residual rl for precise assembly," 2024. [Online]. Available: <https://arxiv.org/abs/2407.16677>
- [16] S. Nair, A. Rajeswaran, V. Kumar, C. Finn, and A. Gupta, "R3m: A universal visual representation for robot manipulation," 2022. [Online]. Available: <https://arxiv.org/abs/2203.12601>
- [17] K. He, X. Zhang, S. Ren, and J. Sun, "Deep residual learning for image recognition," 2015. [Online]. Available: <https://arxiv.org/abs/1512.03385>
- [18] M. Tan and Q. V. Le, "Efficientnet: Rethinking model scaling for convolutional neural networks," 2020. [Online]. Available: <https://arxiv.org/abs/1905.11946>
- [19] K. Simonyan and A. Zisserman, "Very deep convolutional networks for large-scale image recognition," 2015. [Online]. Available: <https://arxiv.org/abs/1409.1556>
- [20] A. Majumdar, K. Yadav, S. Arnaud, Y. J. Ma, C. Chen, S. Silwal, A. Jain, V.-P. Berges, P. Abbeel, F. Malik, D. Batra, Y. Lin, O. Maksymets, A. Rajeswaran, and F. Meier, "Where are we in the search for an artificial visual cortex for embodied intelligence?" 2024. [Online]. Available: <https://arxiv.org/abs/2303.18240>
- [21] A. Howard, M. Sandler, G. Chu, L.-C. Chen, B. Chen, M. Tan, W. Wang, Y. Zhu, R. Pang, V. Vasudevan, Q. V. Le, and H. Adam, "Searching for mobilenetv3," 2019. [Online]. Available: <https://arxiv.org/abs/1905.02244>
- [22] G. Jiang, Y. Sun, T. Huang, H. Li, Y. Liang, and H. Xu, "Robots pre-train robots: Manipulation-centric robotic representation from large-scale robot datasets," 2024. [Online]. Available: <https://arxiv.org/abs/2410.22325>
- [23] A. Dosovitskiy, L. Beyer, A. Kolesnikov, D. Weissenborn, X. Zhai, T. Unterthiner, M. Dehghani, M. Minderer, G. Heigold, S. Gelly, J. Uszkoreit, and N. Houlsby, "An image is worth 16x16 words: Transformers for image recognition at scale," 2021. [Online]. Available: <https://arxiv.org/abs/2010.11929>
- [24] T. Xiao, I. Radosavovic, T. Darrell, and J. Malik, "Masked visual pre-training for motor control," 2022. [Online]. Available: <https://arxiv.org/abs/2203.06173>
- [25] Z. Liu, Y. Lin, Y. Cao, H. Hu, Y. Wei, Z. Zhang, S. Lin, and B. Guo, "Swin transformer: Hierarchical vision transformer using shifted windows," 2021. [Online]. Available: <https://arxiv.org/abs/2103.14030>
- [26] A. Radford, J. W. Kim, C. Hallacy, A. Ramesh, G. Goh, S. Agarwal, G. Sastry, A. Askell, P. Mishkin, J. Clark, G. Krueger, and I. Sutskever, "Learning transferable visual models from natural language supervision," 2021. [Online]. Available: <https://arxiv.org/abs/2103.00020>
- [27] M. Oquab, T. Darcet, T. Moutakanni, H. Vo, M. Szafraniec, V. Khalidov, P. Fernandez, D. Haziza, F. Massa, A. El-Nouby, M. Assran, N. Ballas, W. Galuba, R. Howes, P.-Y. Huang, S.-W. Li, I. Misra, M. Rabbat, V. Sharma, G. Synnaeve, H. Xu, H. Jegou, J. Mairal, P. Labatut, A. Joulin, and P. Bojanowski, "Dinov2: Learning robust visual features without supervision," 2024. [Online]. Available: <https://arxiv.org/abs/2304.07193>
- [28] Y. J. Ma, S. Sodhani, D. Jayaraman, O. Bastani, V. Kumar, and A. Zhang, "Vip: Towards universal visual reward and representation via value-implicit pre-training," 2023. [Online]. Available: <https://arxiv.org/abs/2210.00030>
- [29] M. K. Srirama, S. Dasari, S. Bahl, and A. Gupta, "Hrp: Human affordances for robotic pre-training," 2024. [Online]. Available: <https://arxiv.org/abs/2407.18911>
- [30] K. O'Shea and R. Nash, "An introduction to convolutional neural networks," 2015. [Online]. Available: <https://arxiv.org/abs/1511.08458>
- [31] N. Park and S. Kim, "How do vision transformers work?" 2022. [Online]. Available: <https://arxiv.org/abs/2202.06709>
- [32] K. Grauman, A. Westbury, E. Byrne, Z. Chavis, A. Furnari, R. Girdhar, J. Hamburger, H. Jiang, M. Liu, X. Liu, M. Martin, T. Nagarajan, I. Radosavovic, S. K. Ramakrishnan, F. Ryan, J. Sharma, M. Wray, M. Xu, E. Z. Xu, C. Zhao, S. Bansal, D. Batra, V. Cartillier, S. Crane, T. Do, M. Doulaty, A. Erapalli, C. Feichtenhofer, A. Fragomeni,

- Q. Fu, A. Gebreselasie, C. Gonzalez, J. Hillis, X. Huang, Y. Huang, W. Jia, W. Khoo, J. Kolar, S. Kottur, A. Kumar, F. Landini, C. Li, Y. Li, Z. Li, K. Mangalam, R. Modhugu, J. Munro, T. Murrell, T. Nishiyasu, W. Price, P. R. Puentes, M. Ramazanov, L. Sari, K. Somasundaram, A. Southerland, Y. Sugano, R. Tao, M. Vo, Y. Wang, X. Wu, T. Yagi, Z. Zhao, Y. Zhu, P. Arbelaez, D. Crandall, D. Damen, G. M. Farinella, C. Fuegen, B. Ghanem, V. K. Ithapu, C. V. Jawahar, H. Joo, K. Kitani, H. Li, R. Newcombe, A. Oliva, H. S. Park, J. M. Rehg, Y. Sato, J. Shi, M. Z. Shou, A. Torralba, L. Torresani, M. Yan, and J. Malik, "Ego4d: Around the world in 3,000 hours of egocentric video," 2022. [Online]. Available: <https://arxiv.org/abs/2110.07058>
- [33] J. Yi, B. Kim, and B. Chang, "Embedding normalization: Significance preserving feature normalization for click-through rate prediction," pp. 75–84, 2021. [Online]. Available: <https://doi.org/10.1109/ICDMW53433.2021.00016>
- [34] J. E. Fowler, "Compressive-projection principal component analysis," *IEEE Transactions on Image Processing*, vol. 18, no. 10, pp. 2230–2242, 2009. [Online]. Available: <https://doi.org/10.1109/TIP.2009.2025089>
- [35] K. He, X. Zhang, S. Ren, and J. Sun, "Deep residual learning for image recognition," 2015. [Online]. Available: <https://arxiv.org/abs/1512.03385>
- [36] A. Jaiswal, A. R. Babu, M. Z. Zadeh, D. Banerjee, and F. Makedon, "A survey on contrastive self-supervised learning," *Technologies*, vol. 9, no. 1, 2021. [Online]. Available: <https://www.mdpi.com/2227-7080/9/1/2>